Pramana – J. Phys. (2021) 95:148
https://doi.org/10.1007/s12043-021-02182-1

Strang time-splitting technique for the generalised Rosenau–RLW equation

SELÇUK KUTLUAY[1], MELIKE KARTA[2] and YUSUF UÇAR[1],*

[1]Department of Mathematics, İnönü University, Malatya, Turkey
[2]Department of Mathematics, Ağrı İbrahim Çeçen University, Ağrı, Turkey
*Corresponding author. E-mail: yusuf.ucar@inonu.edu.tr

MS received 11 March 2020; revised 3 October 2020; accepted 3 May 2021

Abstract. In this paper, a numerical scheme based on quintic B-spline collocation method using the Strang splitting technique is presented for solving the generalised Rosenau–regularised long wave (RLW) equation given by appropriate initial-boundary values. For this purpose, firstly the problem is split into two subproblems such that each one includes the derivative in the direction of time. Secondly, each subproblem is reduced to a system of ordinary differential equations (ODEs) using collocation finite-element method with quintic B-splines for spatial integration. Then, the resulting ODEs for time integration are solved using the Strang time-splitting technique with the second order via the usual Runge–Kutta (RK-4) algorithm with the fourth order. To measure the accuracy and efficiency of the present scheme, a model problem with an exact solution is taken into consideration and investigated for various values of the parameter p. The error norms L_2 and L_∞ together with the invariants of discrete mass Q and discrete energy E have been computed and a comparison is given with other ones found in the literature. The convergence order of the present numerical scheme has also been computed. Furthermore, the stability analysis of the scheme is numerically examined.

Keywords. Rosenau–RLW equation; Strang time-splitting; quintic B-splines; collocation; Runge–Kutta; stability analysis.

PACS Nos 2.60.Jv; 12.10.Dm; 98.80.Cq; 11.30.Hv

1. Introduction

There are various nonlinear physical phenomena describing wave behaviours in many applied sciences. One of them is the well-known KdV equation. It is defined as a model for the small amplitude of long waves on the surface of a channel while the regularised long wave (RLW) equation defines the undular bore behaviour. As the KdV equation does not describe the behaviour of wave–wall and wave–wave interactions, Rosenau [1,2] introduced the following Rosenau equation:

$$u_t + u_{xxxxt} + u_x + (u^p)_x = 0. \tag{1}$$

Park [3] gave the existence and uniqueness of the solution of the Rosenau equation. For a further study of the nonlinear waves, the viscous term $-u_{xxt}$ is included in eq. (1) and an equation having a wide application in physics called the Rosenau–RLW equation [4] is obtained.

$$u_t - u_{xxt} + u_{xxxxt} + u_x + (u^p)_x = 0. \tag{2}$$

In the literature, there are several studies for obtaining numerical solutions of the general Rosenau–RLW equation. Among these, Zuo *et al* [5] proposed a nonlinear conservative difference scheme and showed that the scheme is uniquely solvable, unconditionally stable and second-order convergent. Pan and Zhang [6] presented a three-level and linear-implicit finite-difference scheme and also discussed the uniqueness, convergence and stability of the scheme. Pan and Zhang [7] also constructed an energy conservative linearised finite-difference scheme. Meanwhile, they proved that the scheme is uniquely solvable, convergent and stable. Mittal and Jain [8] used a collocation quintic B-splines method. They converted Rosenau–RLW equation into a system of ordinary differential equations (ODEs) using the method for spatial variable and its requried derivatives and then solved it by SSP-RK54 algorithm. Pan *et al* [9] gave a conservative Crank–Nicolson-type numerical scheme. They also showed that the scheme is convergent, stable and uniquely solvable using discrete energy

Published online: 30 August 2021

method. Hu and Wang [10] constructed linear conservative finite-difference scheme with a three-time level and analysed *a priori* estimate in infinite norm, existence and uniqueness of the difference solution. Atouani and Omrani [11] proposed Galerkin–Crank–Nicolson fully discrete method and analysed the boundedness and convergence of the approximate solution. Wongsaijai *et al* [12] presented an average implicit finite-difference scheme with three-time level. Moreover, they proved the convergence and the stability of the numerical solution as well as the existence and uniqueness. Yagmurlu *et al* [13] used Galerkin cubic B-spline finite-element method. They transformed Rosenau–RLW equation into a system of ODEs using the method for space variable and its derivatives, and then solved it using the usual RK-4 algorithm. Moreover, they tested the accuracy of the method by calculating L_2 and L_∞ errors. Wang *et al* [14] presented a linearised conservative difference scheme. They also gave the uniqueness, stability and convergence of the method.

In this study, the generalised Rosenau–RLW equation

$$u_t - \sigma u_{xxt} + \alpha u_{xxxxt} + \gamma u_x + \beta (u^p)_x = 0, \quad (x,t) \in (x_L, x_R) \times (0,T] \tag{3}$$

given by the initial and boundary conditions

$$u(x,0) = u_0(x), \quad x \in [x_L, x_R], \tag{4}$$

$$u(x_L,t) = u(x_R,t) = 0$$

$$u_x(x_L,0) = u_x(x_R,0) = 0; t \in [0,T]$$

$$u_{xx}(x_L,t) = u_{xx}(x_R,t) = 0 \tag{5}$$

is going to be considered. Here $\sigma, \alpha, \gamma, \beta$ and p are positive parameters, $u_0(x)$ is a known smooth function and $[x_L, x_R]$ is the solution domain of the problem. The present paper is outlined as follows. In §2, a brief introduction about time-splitting techniques and especially the Strang one is presented. In §3, quintic B-splines with their derivative values at the collocation nodes are given. This section also deals with the splitting of eq. (3) into two subequations and implementation of the collocation finite-element method with the quintic B-splines. Moreover, in this section the stability of the numerical scheme is also investigated. In §4, some examples are presented and the obtained numerical results using the technique in §2 via the classical fourth-order Runge–Kutta algorithm are given in tables and graphics. Finally, §5 presents a short conclusion.

2. A concise description of Strang time-splitting technique

The splitting techniques are one of the most powerful techniques to solve the abstract Cauchy problems such that their main principle is to convert a given problem into several subproblems solvable on the time intervals $[t_n, t_{n+1}]$. Such methods are commonly referred to as fractional step or time-splitting methods. The method is also called operator splitting if the problem is split up including different physical processes. If a multidimensional problem is decomposed into one-dimensional subproblems then it is called the dimensional splitting [15]. In this study, we concentrate on the second-order Strang time-splitting technique [16–23,25,26]. Second-order splitting methods with higher real coefficients necessarily contain negative coefficients [27]. This situation prevents the use of higher-order methods with real coefficients for equations involving the Laplacian operator defined for positive time. To overcome this situation, high-order methods with complex coefficients with positive real part have been proposed [28]. Such methods are very costly in calculations since they involve the product of complex numbers in practice. On the other hand, second-order high splitting methods cause PDEs to degrade when applied for Dirichlet, Neumann and Robin boundary conditions [29]. For such systems that cannot be inverted in time, it is an advantage to apply the second-order Strang splitting method, as higher-order methods are costly and lead to order decrease. One of the popular methods for solving high-dimensional equations is the operator splitting method to replace a parabolic differential equation in two space dimensions by solving two one-dimensional problems. This basic idea can be extended to split a high-dimensional equation into a system of lower-dimensional equations and solve each low-dimensional equation separately [30]. There are special cases of this splitting procedure. For example, Carbone and Volcic [31] have extended Kakutani's splitting procedure to higher dimensions.

For this purpose, let us consider the following Cauchy problem:

$$u_t = D_1(u) + D_2(u) = D(u), \quad u(0) = u_0, \tag{6}$$

where D_1, D_2 and D are unbounded operators and u_0 is a given function. Obviously, the semi-discretised version of eq. (2) can be written as eq. (6).

The underlying idea behind the time-splitting techniques is to first split eq. (6) into the following two equations:

$$u_t = D_1(u) \quad \text{and} \quad u_t = D_2(u) \tag{7}$$

which can be more easily handled than the original one and can be also solved analytically or approximately. Secondly, each subequation is solved using an appropriate method. In the end, the solution of problem (6) is found by combining the obtained solutions of the subequations (7). Let $S_k^{[1]}$ and $S_k^{[2]}$ be the solution operators of eq. (7) at $t = k$ respectively such that

$u^{[1]}(t+k) = S_k^{[1]}(u(t))$ and $u^{[2]}(t+k) = S_k^{[2]}(u(t))$. Thus, the second-order Strang time-splitting technique can be written in terms of the operators $S_k^{[1]}$ and $S_k^{[2]}$ as follows:

$$u_{n+1} = S_{k/2}^{[1]}(S_k^{[2]}(S_{k/2}^{[1]}(u_n))) \tag{8}$$

with $u(t) \approx u_n$ [24,32].

Any time-splitting technique generally separates a given original problem into two subproblems over a time step. In this study, using the Strang splitting technique for time discretisation and the quintic B-spline collocation finite-element method for space discretisation, each of the subproblems is transformed into an ODE system. Then, the resulting systems are solved with the help of the usual RK-4 algorithm.

The algorithm of Strang technique from (8) is that instead of solving the first subproblem for a full time step k, solve it a half time step $k/2$. Then, solve the second subproblem for a full time step k, and after that back to the first problem and solve it for a half time step $k/2$.

3. Implementation of the method

To implement the method, let the uniform partition of the range $[x_L, x_R]$ be $x_L = x_0 < x_1 < \cdots < x_N = x_R$ and the nodes be x_m, $m = 0(1)N$, $h = x_{m+1} - x_m$. The quintic B-spline basis functions $\varphi_m(x)$ on the solution domain $[x_L, x_R]$ for $m = -2(1)N+2$ at x_m are defined on each consecutive element of the range $[x_{m-3}, x_{m+3}]$ as follows [34]:

$$h^5\varphi_m(x) = \begin{cases} (x-x_{m-3})^5, \\ (x-x_{m-3})^5 - 6(x-x_{m-3})^5, \\ (x-x_{m-3})^5 - 6(x-x_{m-2})^5 \\ \quad +15(x-x_{m-1})^5, \\ (x_{m+3}-x)^5 - 6(x_{m+2}-x)^5 \\ \quad +15((x_{m+1}-x))^5, \\ (x_{m+3}-x)^5 - 6(x_{m+2}-x)^5, \\ (x_{m+3}-x)^5, \\ 0. \end{cases}$$

Outside this range, the quintic B-spline basis function $\varphi_m(x)$ is identically zero. As a typical element $[x_m, x_{m+1}]$ is covered by only six quintic B-splines $\varphi_{m-2}, \varphi_{m-1}, \varphi_m, \varphi_{m+1}, \varphi_{m+2}, \varphi_{m+3}$, the approximate solution $U_N(x,t)$ corresponding to the exact solution $u(x,t)$ of eq. (3) on $[x_m, x_{m+1}]$ can be defined with respect to φ_j and δ_j as follows:

$$u(x,t) \cong U_N^e(x,t) = \sum_{j=m-2}^{m+3} \delta_j(t)\varphi_j(x),$$

where δ_j are time-dependent element parameters to be determined. The values of U_N^e and their consecutive derivatives in the direction of x appearing in eq. (3) at x_m nodes with quintic B-splines can be obtained in terms of δ_m as

$$\begin{aligned} U_N^e(x_m,t) &= U_m = \delta_{m-2} + 26\delta_{m-1} + 66\delta_m \\ &\quad + 26\delta_{m+1} + \delta_{m+2} \\ (U_N^e)_x(x_m) &= U'_m = \frac{5}{h}(-\delta_{m-2} - 10\delta_{m-1} \\ &\quad + 10\delta_{m+1} + \delta_{m+2}) \\ (U_N^e)_{xx}(x_m) &= U''_m \\ &= \frac{20}{h^2}(\delta_{m-2} + 2\delta_{m-1} - 6\delta_m + 2\delta_{m+1} + \delta_{m+2}) \\ (U_N^e)_{xxx}(x_m) &= U'''_m = \frac{60}{h^3}(-\delta_{m-2} + 2\delta_{m-1} \\ &\quad - 2\delta_{m+1} + \delta_{m+2}) \\ (U_N^e)_{xxxx}(x_m) &= U_m^{(4)} \\ &= \frac{120}{h^4}(\delta_{m-2} - 4\delta_{m-1} + 6\delta_m - 4\delta_{m+1} + \delta_{m+2}). \end{aligned} \tag{9}$$

Equation (3) is split into two subequations as follows:

$$u_t - \sigma u_{xxt} + \alpha u_{xxxxt} + \gamma u_x = 0, \tag{10}$$

$$u_t - \sigma u_{xxt} + \alpha u_{xxxxt} + \beta p u^{p-1} u_x = 0. \tag{11}$$

If the values of U_m, U'_m, U''_m, U'''_m and $U_m^{(4)}$ given in eq. (9) are inserted in their places in eqs (10) and (11), a system of ODEs is obtained as follows:

$$\begin{aligned} &\dot\delta_{m-2} + 26\dot\delta_{m-1} + 66\dot\delta_m + 26\dot\delta_{m+1} + \dot\delta_{m+2} \\ &\quad -\sigma\frac{20}{h^2}(\dot\delta_{m-2} + 2\dot\delta_{m-1} - 6\dot\delta_m + 2\dot\delta_{m+1} + \dot\delta_{m+2}) \\ &\quad +\alpha\frac{120}{h^4}(\dot\delta_{m-2} - 4\dot\delta_{m-1} + 6\dot\delta_m - 4\dot\delta_{m+1} + \dot\delta_{m+2}) \\ &\quad +\gamma\frac{5}{h}(-\delta_{m-2} - 10\delta_{m-1} + 104\delta_{m+1} + \delta_{m+2}) = 0, \end{aligned} \tag{12}$$

$$\begin{aligned} &\dot\delta_{m-2} + 26\dot\delta_{m-1} + 66\dot\delta_m + 26\dot\delta_{m+1} + \dot\delta_{m+2} \\ &\quad -\sigma\frac{20}{h^2}(\dot\delta_{m-2} + 2\dot\delta_{m-1} - 6\dot\delta_m + 2\dot\delta_{m+1} + \dot\delta_{m+2}) \\ &\quad +\alpha\frac{120}{h^4}(\dot\delta_{m-2} - 4\dot\delta_{m-1} + 6\dot\delta_m - 4\dot\delta_{m+1} + \dot\delta_{m+2}) \\ &\quad +\frac{5\beta z_m}{h}(-\delta_{m-2} - 10\delta_{m-1} + 10\delta_{m+1} + \delta_{m+2}) = 0, \end{aligned} \tag{13}$$

in which the symbol $'\cdot'$ stands for the first derivative according to time t and z_m is

$$z_m = p(\delta_{m-2}+26\delta_{m-1}+66\dot{\delta}\delta_m + 26\delta_{m+1}+\delta_{m+2})^{p-1}$$

which is to be considered as a local constant. The systems given by eqs (12) and (13) totally include $2\times(N+5)$ unknowns and $2\times(N+1)$ equations. To be able to obtain a solvable system of equations, from each system the fictitious parameters δ_{-2}, δ_{-1} off the left boundary and $\delta_{N+1}, \delta_{N+2}$ off the right boundary standing outside the solution domain are needed to be eliminated. Utilising U and U'' in eq. (9) for the boundary conditions given in eq. (5), the fictitious parameters can be easily eliminated and then the following matrix system in the closed form is obtained:

$$\begin{aligned}\dot{\delta}^{n+1} &= A^{-1}B\delta^n = L_1\delta^n\\ \dot{\delta}^{n+1} &= A^{-1}C\delta^n = L_2\delta^n,\end{aligned} \tag{14}$$

where $\delta^n = (\delta_0, \delta_1, ..., \delta_N)^T$ and the matrices $A = [a_{ij}]$, $B = [b_{ij}]$ and $C = [c_{ij}]$ are of the form $(N+1)\times(N+1)$ having the entries

$$A = \begin{cases} a_{11} = \dfrac{3600\alpha}{h^4},\\ a_{21} = 23+\dfrac{23\sigma}{h^2} - \dfrac{840\alpha}{h^4},\\ a_{22} = 65+\dfrac{140\sigma}{h^2} + \dfrac{600\alpha}{h^4},\\ a_{23} = 26-\dfrac{40\sigma}{h^2} - \dfrac{480\alpha}{h^4},\\ a_{24} = 1-\dfrac{20\sigma}{h^2} + \dfrac{120\alpha}{h^4},\\ a_{i,i-2} = a_{24}, a_{i,i-1} = a_{23},\\ a_{ii} = 66+\dfrac{120\sigma}{h^2}\dfrac{720\alpha}{h^4},\\ a_{i,i+1} = a_{23}, a_{i,i+2} = a_{24};\quad i = 3(1)N-1,\\ a_{N,N-2} = a_{24}, a_{N,N-1} = a_{23},\\ a_{N,N} = a_{22}, a_{N,N+1} = a_{21},\\ a_{N+1,N+1} = a_{11},\end{cases}$$

$$B = \begin{cases} b_{11} = -\dfrac{90\gamma}{h}, b_{12} = -\dfrac{100\gamma}{h}, b_{13} = -\dfrac{10\gamma}{h},\\ b_{21} = \dfrac{35\gamma}{h}, b_{22} = -\dfrac{5\gamma}{h}, b_{23} = -\dfrac{50\gamma}{h},\\ b_{24} = -\dfrac{5\gamma}{h},\\ b_{i,i-2} = -b_{22}, b_{i,i-1} = -b_{23}, b_{ii} = b_{23},\\ b_{i,i+1} = b_{22};\quad i = 3(1)N-1,\\ b_{N,N-2} = -b_{22},\ b_{N,N-1} = -b_{23},\\ b_{N,N} = -b_{22}, b_{N,N+1} = -b_{21},\\ b_{N+1,N-1} = -b_{13} b_{N+1,N} = -b_{12},\\ b_{N+1,N+1} = -b_{11},\end{cases}$$

$$C = \begin{cases} c_{1i} = 0;\quad i = 1(1)N+1,\\ c_{21} = \dfrac{35\beta z_1}{h}, c_{22} = -\dfrac{5\beta z_1}{h},\\ c_{23} = -\dfrac{50\beta z_1}{h}, c_{24} = -\dfrac{5\beta z_1}{h},\\ c_{i,i-2} = \dfrac{35\beta z_i}{h}, c_{i,i-1} = \dfrac{50\beta z_i}{h},\\ c_{ii} = 0, c_{i,i+1} = -\dfrac{50\beta z_i}{h},\\ c_{i,i+1} = -\dfrac{5\beta z_i}{h};\quad i = 3(1)N-1,\\ c_{N,N-2=}\dfrac{5\beta z_N}{h},\ c_{N,N-1=}\dfrac{50\beta z_N}{h},\\ c_{N,N=}\dfrac{5\beta z_N}{h}, c_{N,N+1=}\dfrac{35\beta z_N}{h},\\ c_{N+1,i} = 0;\quad i = 1(1)N+1.\end{cases}$$

Now the ODE system given in eq. (14) is solved for the time integration by the Strang time-splitting technique (8) by virtue of the usual RK-4 algorithm. To get better results, an iteration given by $(\delta^*)^{n+1} = \delta^n + 1/2(\delta^{n+1} - \delta^n)$ has been applied 3–5 times at every time step to the nonlinear term z_m in eq. (13) during the run-time.

For the solution of systems (12) and (13), an initial vector δ_m^0 is needed. This vector can be calculated using the initial condition (4)

$$u(x_m, 0) = u_0(x_m) = U(x_m, 0), \quad m = 0(1)N$$

and the boundary conditions (5)

$$\begin{aligned}u_x(x_L, 0) &= u_x(x_R, 0) = 0\\ u_{xx}(x_L, 0) &= u_{xx}(x_R, 0) = 0.\end{aligned}$$

Therefore, the initial vector δ_m^0 is obtained as follows:

$$\begin{bmatrix} 54 & 60 & 6 & & & & & \\ 25.25 & 67.5 & 26.25 & 1 & & & & \\ 1 & 26 & 66 & 26 & 1 & & & \\ & & & \ddots & & & & \\ & & 1 & 26 & 66 & 26 & 1 & \\ & & & 1 & 26.25 & 67.5 & 25.25 & \\ & & & & 6 & 60 & 54 & \end{bmatrix} \begin{bmatrix} \delta_0^0 \\ \delta_1^0 \\ \delta_2^0 \\ \vdots \\ \delta_{N-2}^0 \\ \delta_{N-1}^0 \\ \delta_N^0 \end{bmatrix} = \begin{bmatrix} u_0 \\ u_1 \\ u_2 \\ \vdots \\ u_{N-2} \\ u_{N-1} \\ u_N \end{bmatrix}.$$

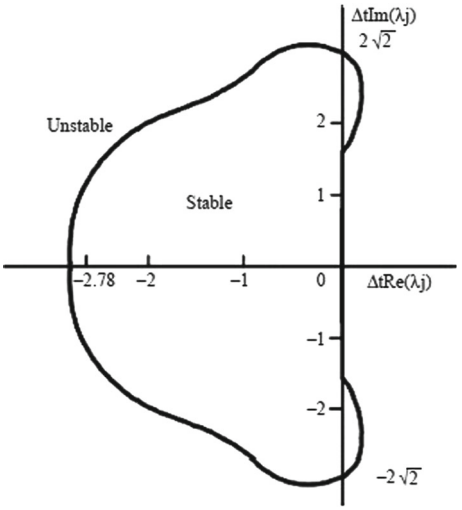

Figure 1. The stability region for the RK-4 method.

3.1 *Stability analysis*

The Strang time-splitting scheme for eq. (14) can be written as

$$\begin{aligned}\dot{\delta}^{n+1} &= L_1\delta^n,\\ \dot{\delta}^{n+1} &= L_2\delta^n,\\ \dot{\delta}^{n+1} &= L_1\delta^n.\end{aligned} \tag{15}$$

Assume that the combined coefficient matrix of the system given by eq. (15) is of the form

$$L = \begin{bmatrix} L_1 & & \\ & L_2 & \\ & & L_1 \end{bmatrix}. \tag{16}$$

Now, let us investigate numerically the stability analysis of the scheme given by eq. (15). For this, it is sufficient to examine the eigenvalues λ_i of the matrix L given by (16). From ref. [33], the RK-4 method is stable if and only if

(i) $-2.78 < \lambda_i \Delta t < 0$ for real λ_i

(ii) $-2\sqrt{2} < \lambda_i \Delta t < 2\sqrt{2}$ for pure imaginary λ_i

(iii) $\lambda_i \Delta t$ for complex λ_i belongs to the region illustrated in figure 1. In the case of complex eigenvalues, there exists a tolerance range where the real parts of the eigenvalues belong.

The eigenvalues λ_i of matrix L for selecting the values of Δt in the numerical experiments considered at the end of the next section have been calculated using MATLAB and illustrated graphics. It is observed from the obtained values of $\lambda_i \Delta t's$ that the above stability criteria are satisfied. So, the numerical scheme (15) is stable. For a more detailed proof of the stability analysis of the Runge–Kutta method, the readers can read refs [36–38] and references therein.

4. Numerical experiments and results

To show how good is the numerical results obtained by the present method, the error norms L_2 and L_∞ are given as

$$L_2 = \left[h \sum_{j=1}^{N} |u_j^{\text{exact}} - U_j|^2 \right]^{1/2},$$

$$L_\infty = \max_j |u_j^{\text{exact}} - U_j|$$

with the following conservation constants $Q(t)$ and $E(t)$ of the problem given by eqs (3)–(5):

$$\begin{aligned} Q(t) &= \int_{x_L}^{x_R} u(x,t)dx \; (= Q(0)) \\ &\simeq h \sum_{j=1}^{N-1} U_j \end{aligned} \tag{17}$$

$$\begin{aligned} E(t) &= \int_{x_L}^{x_R} [u^2(x,t) + u_x^2(x,t) + u_{xx}^2(x,t)]\mathrm{d}x \; (= E(0)) \\ &\simeq h \sum_{j=1}^{N-1} [(U_j)^2 + ((U_j)_x)^2 + ((U_j)_{xx})^2] \end{aligned}$$

and the convergence order given by

$$\text{Order} = \log_2(L(2h, 2\Delta t)/L(h, \Delta t))$$

are calculated. Here L is either L_2 or L_∞, and both h and Δt are sufficiently small.

For all calculations, the software MATLAB R2011a is used on Intel machine having a memory 4 GB.

Rosenau–RLW equation (3) for $\alpha = \sigma = \beta = \gamma = 1$ has an exact solution of the form [35]

$$u(x,t) = \exp\left[\frac{\ln \frac{(p+3)(3p+1)(p+1)}{2(p^2+3)(p^2+4p+7)}}{p-1} \right] \times \operatorname{sech}^{\frac{4}{p-1}} \left[\frac{(p-1)}{\sqrt{4p^2+8p+20}}(x-ct) \right]$$

where

$$c = \frac{p^4+4p^3+14p^2+20p+25}{p^4+4p^3+10p^2+12p+21}.$$

In all the numerical experiments, for comparing with some studies available in the literature, all computations have been done using the same parameters.

Case 1: In this case, we take $p = 2$ and $[x_L, x_R] = [-30, 30]$. The error norm L_∞ found by the present numerical scheme is listed and compared with the values given in ref. [6] for $h = \Delta t = 0.1$ from $t = 2$ to $t = 10$ with time increment 2 in table 1. One can clearly see from the table that our results are sufficiently small which establish that the numerical and exact solutions

Table 1. Error norm L_∞ for Case 1 ($p = 2$, $h = \Delta t = 0.1$, $[x_L, x_R] = [-30, 30]$).

	Present	[6] ($\theta = 1$)
t	$L_\infty \times 10^5$	$L_\infty \times 10^5$
2	0.2528	1.7282
4	0.6252	3.3671
6	2.5497	4.8067
8	10.3546	10.3546
10	41.7005	41.7005

Table 2. Error norms L_2 and L_∞ for Case 2 ($p = 2$, $h = \Delta t = 0.1$, $[x_L, x_R] = [-30, 120]$).

	Present		[8]	
t	$L_2 \times 10^5$	$L_\infty \times 10^6$	$L_2 \times 10^5$	$L_\infty \times 10^6$
2	0.5194	2.5278	0.5822	2.8908
4	0.9656	4.5794	1.0632	5.1694
6	1.3106	5.8405	1.4223	6.4804
8	1.5662	6.6311	1.6523	7.1646
10	1.7569	7.1795	1.8123	7.6292

are very close to each other. Also, by comparing with the method used in ref. [6], our numerical scheme produces better error estimates. One can easily observe that for the range $[x_L, x_R] = [-30, 30]$ the maximum error has taken place near the right boundary with the increasing time since the range is not large enough to exhibit the correct physical behaviour of the initial-boundary value problem considered in this paper.

Case 2: For this experiment, we again take $p = 2$ but over the range $[x_L, x_R] = [-30, 120]$. Table 2 gives comparison of error norms L_2 and L_∞ obtained by our numerical scheme with those of the method in ref. [8] for $h = \Delta t = 0.1$ from $t = 2$ to $t = 10$ with time increment 2. One can see that our results are slightly better than those in ref. [8]. The error norms L_2 and L_∞ are also calculated over the range $[x_L, x_R] = [-30, 120]$ for $\Delta t = 0.1$ and various space step sizes of h at $t = 10$ and compared with the results of ref. [8] in table 3. As can be seen from the table, our scheme produces better results than the method in ref. [8] and both errors decrease as h decreases.

Case 3: In this case, we take $p = 4$ and $[x_L, x_R] = [-30, 120]$. Table 4 gives a comparison of the error norms L_2 and L_∞ obtained by the presented numerical scheme for $\Delta t = 0.1$ and various space step sizes of h at $t = 60$ with those of the method given in ref. [8]. One can see from the table that the results given in ref. [8] are slightly better than our results, but our error

Table 3. Error norms L_2 and L_∞ for Case 2 ($p = 2$, $\Delta t = 0.1$, $[x_L, x_R] = [-30, 120]$, $t = 10$).

	Present		[8]	
h	$L_2 \times 10^4$	$L_\infty \times 10^4$	$L_2 \times 10^4$	$L_\infty \times 10^4$
0.5	4.5205	1.8971	4.5438	1.9117
0.25	1.1206	0.4693	1.1308	0.4761
0.125	0.2764	0.1145	0.2829	0.1191
0.0625	0.0683	0.0256	0.0716	0.0299

Table 4. Error norms L_2 and L_∞ for Case 3 ($p = 4$, $\Delta t = 0.1$, $[x_L, x_R] = [-30, 120]$, $t = 60$).

	Present		[8]	
h	$L_2 \times 10^2$	$L_\infty \times 10^2$	$L_2 \times 10^2$	$L_\infty \times 10^2$
1.0	2.0799	0.8308	3.0217	1.1541
0.5	0.5136	0.2054	0.5585	0.2216
0.25	0.1316	0.0523	0.1301	0.0518
0.125	0.0388	0.0142	0.0351	0.0128
0.0625	0.0205	0.0046	0.0182	0.0032

Table 5. Error norms L_2 and L_∞ for Case 4 ($p = 2, h = \Delta t = 0.1$, $[x_L, x_R] = [-30, 120]$.

	Present		[8]	
t	$L_2 \times 10^5$	$L_\infty \times 10^5$	$L_2 \times 10^5$	$L_\infty \times 10^5$
10	1.7569	0.7180	1.8132	0.7629
20	2.2618	0.8634	2.2513	0.9095
30	2.5020	0.9419	2.5463	1.0274
40	2.6567	0.9994	2.8139	1.1378
50	2.7735	1.0470	3.0753	1.2447
60	2.8718	1.0897	3.3375	1.3495
	$L_2 \times 10^3$	$L_\infty \times 10^3$		
60 [5]	3.4743	1.2522		
60 [35]	–	0.1912		

norms are sufficiently small and both errors decrease as h decreases.

Case 4: For this experiment, we take $p = 2$ and $[x_L, x_R] = [-30, 120]$. The error norms calculated by our scheme for $h = \Delta t = 0.1$ at some selected times up to $t = 60$ are listed in table 5 with those given in refs [5,8,35]. As can be seen in table 5, our results at each time are slightly better than those in ref. [8] and much more better than those in ref. [5,35] at $t = 60$.

Case 5: In this case, we take $p = 2$ and $[x_L, x_R] = [-40, 60]$. Table 8 compares the error norms L_2 and L_∞ with those given in ref. [9] for various mesh step sizes of $h = \Delta t$ at $t = 10$, 20. It is clearly seen from

Table 6. Error norms L_2 and L_∞ for Case 6 ($p = 3, h = \Delta t = 0.1, [x_L, x_R] = [-30, 120]$).

	Present		[8]	
t	$L_2 \times 10^4$	$L_\infty \times 10^5$	$L_2 \times 10^4$	$L_\infty \times 10^5$
10	0.4910	2.1511	0.4941	2.1569
20	0.6931	2.8701	0.6531	2.7517
30	0.8613	3.5042	0.8000	3.3326
40	1.0236	4.1167	0.9479	3.9091
50	1.1855	4.7239	1.0984	4.4846
60	1.3484	5.3277	1.2513	5.0589
	$L_2 \times 10^3$	$L_\infty \times 10^3$		
60 [5]	7.3571	2.7090		
60 [35]	–	0.3849		

Table 7. Error norms L_2 and L_∞ for Case 7 ($p = 6, h = \Delta t = 0.1, [x_L, x_R] = [-30, 120]$).

	Present		[8]	
t	$L_2 \times 10^3$	$L_\infty \times 10^4$	$L_2 \times 10^3$	$L_\infty \times 10^4$
10	0.6542	3.0980	0.6600	3.1032
20	1.1404	3.1897	1.1382	3.1897
30	1.4673	3.2756	1.4631	3.2836
40	1.7255	3.4099	1.7187	3.4181
50	1.9468	3.4115	1.9368	3.4127
60	2.1422	3.3622	2.1280	3.3650
	$L_2 \times 10^2$	$L_\infty \times 10^3$		
60 [5]	1.1569	4.1593		
60 [35]	–	1.8246		

the table that our scheme performs much better than the other one and produces considerable reductions in the errors for smaller mesh step sizes. The table also shows the convergence order of the present scheme. One can obviously see from the table that the calculated convergence order of the scheme is about 2 which verifies its analytical value 2.

Case 6: For this experiment, we take $p = 3$ and $[x_L, x_R] = [-30, 120]$. Table 6 gives the error norms L_2 and L_∞ for $h = \Delta t = 0.1$ at some selected times up to $t = 60$. This table also presents the comparison of our results with those of refs [5,8,35] for the same parameters. As can be seen in table 6, our results are considerably small and much better than those given in refs [5,35]. But the method in ref. [8] produces slightly better results than our scheme.

Case 7: In this case, we take $p = 6$ and $[x_L, x_R] = [-30, 120]$. Table 7 gives a comparison of the error norms L_2 and L_∞ computed by our numerical scheme for $h = \Delta t = 0.1$ at some selected times up to $t = 60$ with those of refs [5,8,35]. One can clearly see from the table that our results are in sufficiently good agreement with those given in ref. [8] and much better than those given in refs [5,35].

Case 8: For this experiment, to make a comparison with ref. [10], we take $p = 2$ and $\beta = 1/2$ in eq. (3). With these parameters, the exact solution of eq. (3) is [5]

$$u(x,t) = \frac{15}{19}\text{sech}^4\left[\frac{1}{2\sqrt{13}}\left(x - \frac{169}{133}t\right)\right].$$

Table 9 compares the error norms L_2 and L_∞ obtained by our numerical scheme with those from ref. [10] over the range $[x_L, x_R] = [-50, 100]$ for various step sizes of Δt and h at some selected times up to $t = 40$. One can see from the table that our all error norms decrease as h and Δt decrease and are emarkably better than those in ref. [10]. Table 10 gives a comparison of the discrete values of conservation properties $E(t)$ and $Q(t)$ obtained by the presented scheme with those given in ref. [10] and analytical values obtained from eq. (17). It is clearly seen from the table that all the given results are considerably very close to each other and invariants $E(t)$ and $Q(t)$ preserve with the time increasing.

Figure 2 displays the wave profiles of the exact solution at time $t = 0$ and numerical solutions at various times with $h = \Delta t = 0.1$ over the range $[x_L, x_R] = [-30, 120]$ for $p = 2, 3, 4$ and 6. Since the exact and numerical solutions are very close to each other, their graphs are indistinguishable in the figure. It is seen from the figure that the wave profiles at various times are in very good agreement with those at $t = 0$ which obviously shows the efficiency of the numerical scheme given by eq. (15).

In order to show numerically satisfying stability criteria of the presented scheme, the graphics of the eigenvalues λ_i of coefficient matrix corresponding to the scheme multiplied by Δt are respectively given in figures 3 and 4 for Cases 1 and 2 only. From the figures, it is obviously seen that the values $\lambda_i \Delta t$ lie on the RK-4 stability region. One can observe that the values $\lambda_i \Delta t$ for other cases also lie on the RK-4 stability region.

5. Conclusion and further work

In this research work, for the numerical solutions of a test problem for the Rosenau–RLW equation subject to the appropriate initial-boundary conditions, the problem is firstly split in temporal direction into two subproblems and then the resulting ODE system is discretised using quintic B-spline collocation finite-element method for space integration. The obtained semi-discretised ODE system is solved using Strang time-splitting technique for time integration via the fourth-order RK-4 method.

Table 8. L_2 and L_∞ error norms and convergence order for Case 5 ($p = 2$, $h = \Delta t$, $[x_L, x_R] = [-40, 60]$).

		Present				[9]	
t	Δt	$L_2 \times 10^4$	$L_\infty \times 10^4$	Order (L_2)	Order (L_∞)	$L_2 \times 10^4$	$L_\infty \times 10^4$
10	0.2	1.4054	0.5745	–	–	18.0681	7.6481
	0.1	0.3510	0.1436	2.0014	2.0002	4.5278	1.9192
	0.05	0.0877	0.0359	2.0008	2.0000	1.1326	0.4801
	0.025	0.0219	0.0090	2.0016	1.9960	–	–
20	0.2	1.8083	0.6915	–	–	34.5469	14.2582
	0.1	0.4516	0.1727	2.0015	2.0015	8.6612	3.5757
	0.05	0.1129	0.0432	2.0000	1.9992	2.1668	0.8947
	0.025	0.0283	0.0108	1.9962	2.0000	–	–

Table 9. L_2 and L_∞ error norms for Case 8 ($p = 2$, $[x_L, x_R] = [-50, 100]$).

			Present		[10]	
h	Δt	t	$L_2 \times 10^3$	$L_\infty \times 10^3$	$L_2 \times 10^3$	$L_\infty \times 10^3$
0.2	0.4	10	0.1434	0.0472	9.4960	3.5273
		20	0.2130	0.0622	15.5880	5.3831
		30	0.2437	0.0661	19.0199	6.2327
		40	0.2594	0.0676	20.8332	6.5588
			$L_2 \times 10^4$	$L_\infty \times 10^4$	$L_2 \times 10^4$	$L_\infty \times 10^4$
0.1	0.1	10	0.3512	0.1435	5.8708	2.1867
		20	0.4526	0.1728	9.6592	3.3204
		30	0.5018	0.1891	11.7616	3.8368
		40	0.5345	0.2014	12.8693	4.0327
			$L_2 \times 10^5$	$L_\infty \times 10^5$	$L_2 \times 10^5$	$L_\infty \times 10^5$
0.05	0.025	10	0.8928	0.3740	3.6799	1.3711
		20	1.1193	0.4474	6.0281	2.0733
		30	1.2564	0.5010	7.3263	2.3891
		40	1.3726	0.5492	8.0041	2.5035

Table 10. Discrete mass Q and discrete energy E for Case 8 ($p = 2$, $[x_L, x_R] = [-50, 100]$).

			Present		[10]	
h	Δt	t	Q	E	Q	E
0.2	0.4	0	7.59063426412	4.26542026069	7.59537171309	4.26542015423
		10	7.59059732947	4.26538618320	7.59537171275	4.26558683637
		20	7.59056040001	4.26535210516	7.59537171886	4.26577432049
		30	7.59052347140	4.26531801186	7.59537132913	4.26590472629
		40	7.59048654444	4.26522839129	7.59537390280	4.26598379748
0.1	0.1	0	7.59063311017	4.26542025662	7.59093169500	4.26542024995
		10	7.59063368723	4.26541972638	7.59093168588	4.26542086750
		20	7.59063311017	4.26541919528	7.59093167701	4.26542158265
		30	7.59063253306	4.26541866395	7.59093166975	4.26542206996
		40	7.59063195590	4.26541813254	7.59093166785	4.26542236189
0.05	0.025	0	7.59063426411	4.26542025637	7.59065285879	4.26542015595
		10	7.59063425524	4.26542024813	7.59065230880	4.26541966402
		20	7.59063424630	4.26542023981	7.59065176013	4.26541907347
		30	7.59063423737	4.26542023149	7.59065121035	4.26541848035
		40	7.59063422844	4.26542022319	7.59065066159	4.26541788802

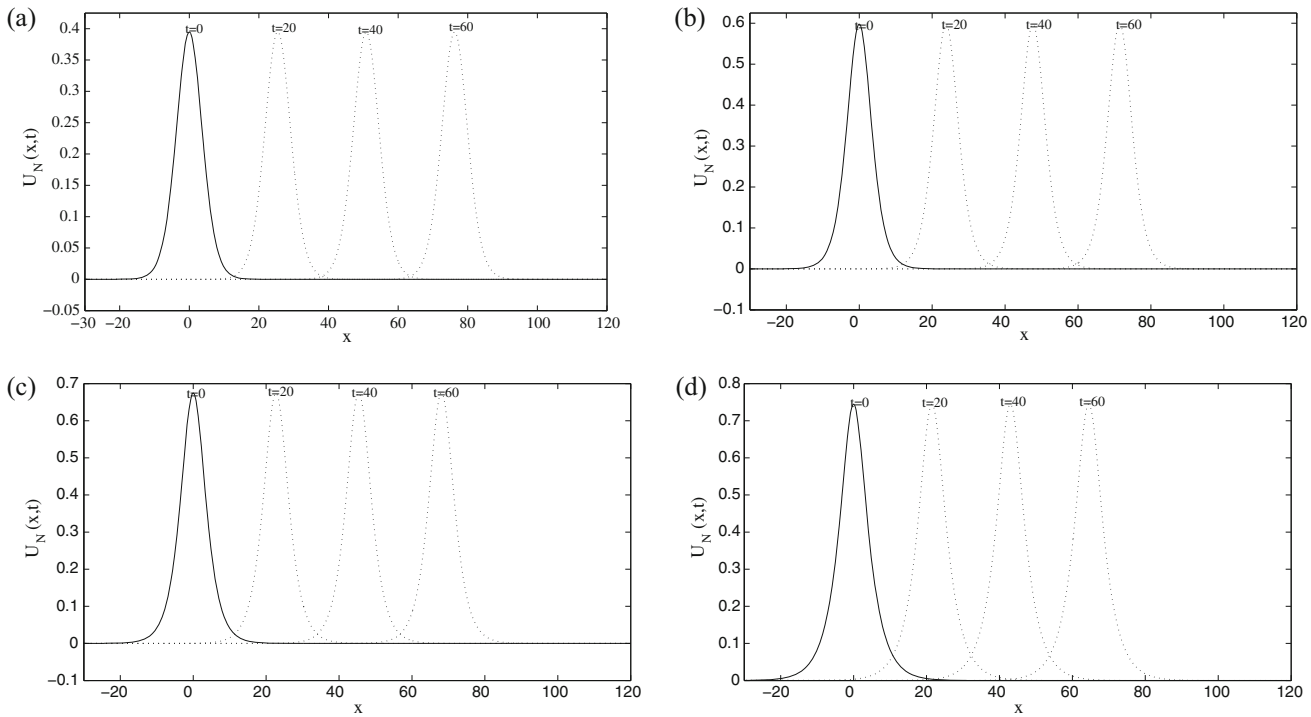

Figure 2. The wave profiles of the exact solution at $t = 0$ and numerical solutions at various times with $h = \Delta t = 0.1$ over the range $[x_L, x_R] = [-30, 120]$ for (**a**) $p = 2$, (**b**) $p = 3$, (**c**) $p = 4$ and (**d**) $p = 6$.

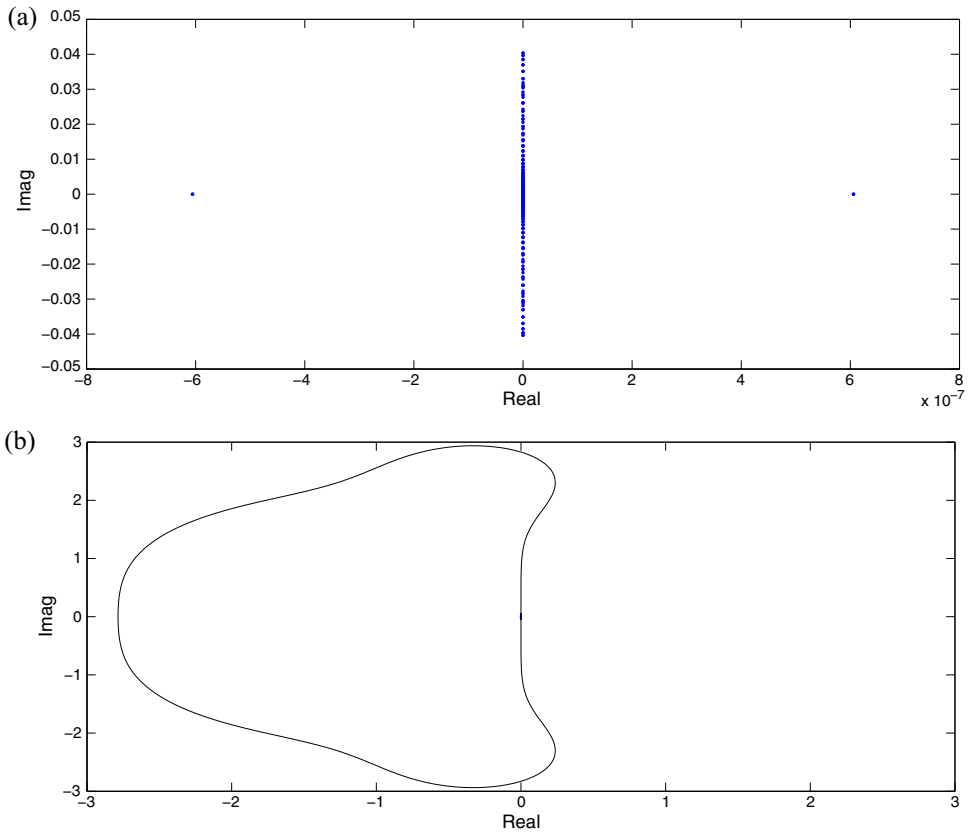

Figure 3. (**a**) The eigenvalues multiplied by Δt for Case 1 in complex coordinate system and (**b**) the eigenvalues inside the stability region for RK-4 method.

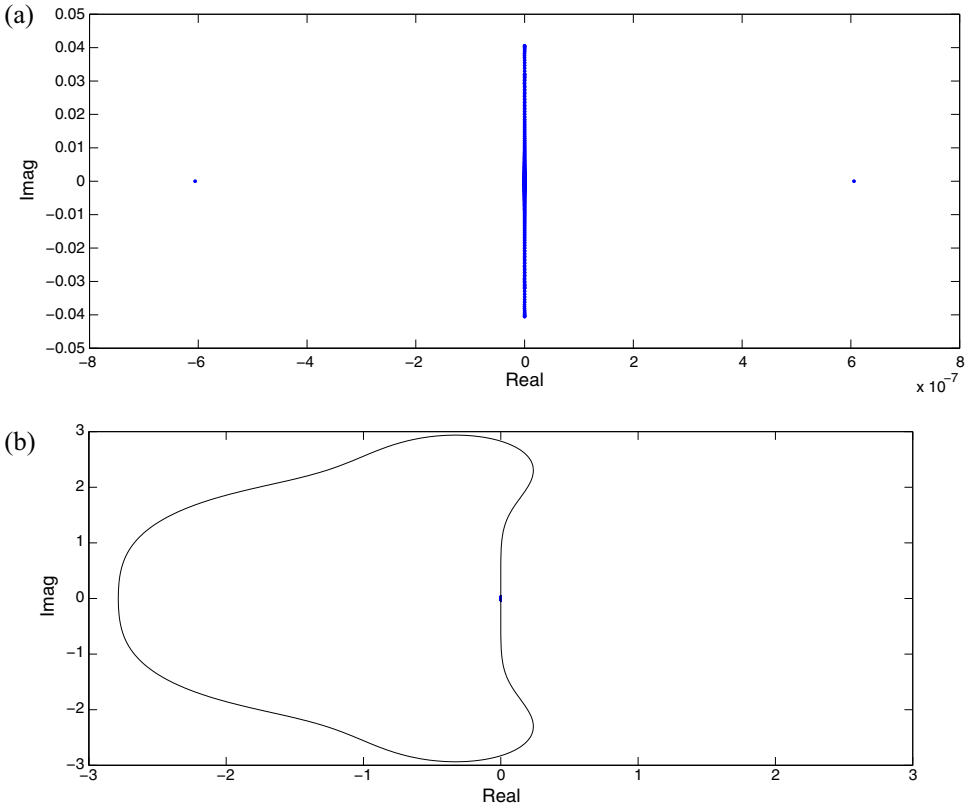

Figure 4. (**a**) The eigenvalues multiplied by Δt for Case 2 in complex coordinate system and (**b**) the eigenvalues inside the stability region for RK-4 method.

For the test problem depending on various choices of the parameter p, the error norms L_2 and L_∞, the conservation constants of discrete energy E and discrete mass Q with the convergence order of the scheme are calculated and compared with some results existing in the literature. The obtained numerical results indicate that the error norms L_2 and L_∞ are sufficiently small, the conservation constants are preserved and nearly constant for long computing time and the convergence order of the scheme is very compatible with its analytical value. As a conclusion, the present scheme produces quite satisfactory results, comparable with the available solutions found in the literature. Thus, it can be successfully used to obtain numerical solutions of these types of problems occurring in engineering and science.

As a further work, the predictions and algorithms presented in this article can be extended to higher-dimensional problems and applied similarly to the one-dimensional problem. However, while the calculation cost of the Strang splitting technique used for the time discretisation in such problems does not change significantly, the calculation cost of the quintic B-spline collocation finite-element method used for the space discretisation increases as the dimension number increases.

Acknowledgements

The authors would like to express their sincere thanks to referees and editor for their many valuable suggestions and comments to improve the quality of the paper.

References

[1] P Rosenau, *Phys. Scr.* **34,** 827 (1986)
[2] P Rosenau, *Progr. Theoret. Phys.* **79**, 1028 (1988)
[3] M A Park, *Mat. Aplic. Comp.* **9**, 145 (1990)
[4] J M Zuo, Y M Zhang, T D Zhang and F Chang, *Bound. Value Probl.* **2010**, 13 (2010)
[5] J M Zuo, Y M Zhang, T D Zhang and F Chang, *Bound. Value Probl.* **2010**, 13 (2010)
[6] X Pan and L Zhang, *Appl. Math. Model*. **36**, 3371 (2012)
[7] X Pan and L Zhang, *Math. Prob. in Eng*. **2012**, 15 (2012)
[8] R C Mittal and R K Jain, *Commun. Numer. Anal.* **2012,** 16 (2012)
[9] X Pan, K Zheng and L Zhang, *Appl. Anal*. **92**, 2578 (2013)
[10] J Hu and Y Wang, *Math. Prob. Eng*. **2013**, 8 (2013)
[11] N Atouani and K Omrani, *Comput. Math. Appl.* **66**, 289 (2013)
[12] B Wongsaijai, K Poochinapan and T Disyadej, *Int. J. Appl. Math*. **44(4)**, 5 (2014)

[13] N M Yagmurlu, B Karaagac and S Kutluay, *Am. J. Comput. Appl. Math.* **7(1)**, 1 (2017)
[14] H Wang, S Li and J Wang, *Comput. Appl. Math.* **36**, 63 (2017)
[15] W Hundsdorfer, *Lecture notes for Ph.D. course* (Thomas Stieltjes Institute, Amsterdam, 2000)
[16] B Gustafsson, High order difference methods for time dependent PDE, in: *Springer series in computational mathematics* (Springer-Verlag, Berlin, New York, Heidelberg, 2007) p. 38
[17] M D Buhlmann, Radial basis functions, in: *Cambridge monographs on applied and computational mathematics* (Cambridge, 2004)
[18] J Geiser and K Bartecki, *AIP Conf. Proc*. **470002**, 1978 (2018)
[19] J Geiser, Decomposition methods for differential equations: Theory and applications, in: *Chapman & Hall/CRC numerical analysis and scientific computing series* (Chapman & Hall, New York, 2009)
[20] J Geiser and A Nasari, *Math. Comput. Appl*. **24**, 76 (2019)
[21] J Geiser, *Multicomponent and multiscale systems – Theory, methods, and applications in engineering* (Springer International Publishing, AG, 2016)
[22] G Strang, *SIAM J. Numer. Anal.* **5**, 506 (1968)
[23] R I McLachlan and G R W Quispel, *Acta Numer.* **2001**, 341 (2001)
[24] S Blanes and F Casas, *A concise introduction to geometric numerical integration* (CRC Press, 2016)
[25] J Geiser, *J. Algorithm Comput. Technol.* **9(1)**, 65 (2013)
[26] G I Marchuk, *Appl. Math.* **13**, 103 (1968)
[27] S Blanes and F Kasas, *Appl. Numer. Meth*. **54**, 23 (2005)
[28] M Seydaoğlu and S Blanes, *Appl. Numer. Meth*. **84**, 22 (2014)
[29] M Seydaoğlu, U Erdogan and T Oziş, *J. Comput. Appl. Math.* **291**, 410 (2016)
[30] S Ganesan and L Tobiska, *Appl. Math. Comput*. **219**, 6182 (2013)
[31] I Carbone and A Volcic, *Rend. Istit. Mat. Univ. Trieste* **XXXIX**, 119 (2007)
[32] F Zürnacı and M Seydaoğlu, *Numer. Meth. Part. D E* **35(1)**, 1363 (2019)
[33] W Hundsdorfer and J Verwer, *Numerical solution of time-dependent advection-diffusion-reaction equations* (Springer-Verlag, Berlin, Heidelberg, 2003)
[34] P M Prenter, *Splines and variational methods* (Wiley, New York, 1975)
[35] H Wang, J Wang and S Li, *Bound. Value Probl.* **2015**, 11 (2015)
[36] S Kutluay, M Karta and N M Yağmurlu, *Numer. Meth. Part. D E* **35**, 2221 (2019)
[37] Abbas I Abdel Karim, *Comput. J*. **9(3)**, 308 (1966)
[38] John W Carr, *J. Assoc. Comp. Mach*. **5(1)**, 39 (1958)